

Strain and Water Effects on the Electronic Structure and Chemical Activity of In-Plane Graphene/Silicene Heterostructure

Andrey A Kistanov^{1,2,*}, Yongqing Cai², Yong-Wei Zhang^{2,*}, Sergey V Dmitriev^{3,4} and Kun Zhou^{1,*}

¹School of Mechanical and Aerospace Engineering, Nanyang Technological University, 639798 Singapore

²Institute of High Performance Computing, Agency for Science, Technology and Research, 138632 Singapore

³Institute for Metals Superplasticity Problems, Russian Academy of Sciences, 450001 Ufa, Russia

⁴Research Laboratory for Mechanics of New Nanomaterials, Peter the Great St. Petersburg Polytechnical University, 195251 St. Petersburg, Russia

*E-mail: kzhou@ntu.edu.sg (K. Z.), andrei.kistanov.ufa@gmail.com (A. A. K.) and zhangyw@ihpc.a-star.edu.sg (Y.-W. Z.)

Abstract

By using first-principles calculations, the electronic structure of planar and strained in-plane graphene/silicene heterostructure is studied. The heterostructure is found to be metallic in a strain range from -7% (compression) to +7% (tension). The effect of compressive/tensile strain on the chemical activity of the in-plane graphene/silicene heterostructure is examined by studying its interaction with the H₂O molecule. It shows that compressive/tensile strain is able to increase the binding energy of H₂O compared with the adsorption on a planar surface, and the charge transfer between the water molecule and the graphene/silicene sheet can be modulated by strain. Moreover, the presence of the boron-nitride (BN)-substrate significantly influences the chemical activity of the graphene/silicene heterostructure upon its interaction with the H₂O molecule and may cause an increase/decrease of the charge transfer between the H₂O molecule and the heterostructure. These findings provide insights into the modulation of electronic properties of the in-plane free-standing/substrate-supported graphene/silicene heterostructure, and render possible ways to control its electronic structure, carrier density and redox characteristics, which may be useful for its potential applications in nanoelectronics and gas sensors.

Keywords: graphene, silicene, in-plane heterostructure, chemical activity, strain and water effects, BN-substrate

1. Introduction

Since its first fabrication in 2004 [1], graphene, a two-dimensional (2D) single atomic layer of crystalline carbon, has been intensively investigated because of its unique opto-electronic and mechanical properties, such as a high carrier mobility [2] of $200,000 \text{ cm}^2/\text{Vs}$, an extraordinarily high Young's modulus [3] of 1.0 TPa and extra flexibility [4]. Recently produced silicene [5], a 2D allotrope of silicon, is also an important material among other 2D materials. Similar to graphene, silicene is a zero-gap semiconductor with a tunable band gap [6]. In addition, silicene possesses a high intrinsic carrier mobility [7] of $2.57 \cdot 10^5 \text{ cm}^2/\text{V}\cdot\text{s}$, and suitable mechanical flexibility [8]. These extraordinary properties suggest silicene as another promising material for novel device applications. However, constraints like the absence of the band gap, and poor mechanical properties of silicene have driven researchers to seek other novel materials. Over the past few years, many researches have been focused on hybrid 2D materials, such as graphene/hexagonal-boron-nitride (h-BN) [9, 10], graphene/transition metal dichalcogenide (TMD) [11, 12], h-BN/silicene [13], and graphene/silicene heterostructures [14]. These 2D heterostructures are designed to overcome limitations and to develop the performance of individual 2D materials [15–19].

Furthermore, because of its atomically thin structure and large surface area, 2D materials such as silicene are easily subjected to exposure of the environment, and their electronic properties can be greatly affected by it [20, 21]. To protect chemically unstable 2D materials, commonly, passivation by using more stable 2D materials, such as graphene or h-BN, as a capping layer is used [22, 23]. However, manufacturing of vertically stacked materials has disadvantages, due to the possible contamination between layers, which leads to significant challenges for massive production of the samples [24, 25]. In that case, the in-plane interconnected heterostructures, for which there are no such issues in their production, have attracted great attentions from both theoretical and experimental sides [26, 27].

Recently, many studies have reported on the effect of various factors on the electronic properties of different heterostructures [9, 28–30]. For example, electric-field engineering was applied to modify the band gap of graphene/h-BN heterostructures [31]. The works [32, 33] predicted that despite that the differences in the electronic and mechanical properties of graphene/silicene heterostructure under different types of applied strain may exist, for a gas adsorption at sites far away from the interface region, the type of strain applied is expected to exert little effect due to the nearly isotropic nature of both graphene and silicene sheets. Doping of graphene/silicon junction solar cells led to a significant enhancement, up to 3.9%, of energy conversion

efficiency [34]. Strain engineering was found as an effective way to change the band gap of heterostructures. In addition, mechanically-tuned band gap was predicted in graphene/h-BN [30, 31, 34, 35] and graphene/MoS₂ heterostructures [36, 37]. However, it is noted that the strain effects on the in-plane graphene/silicene heterostructure remain unexplored.

In this work, we perform investigations on the effects of strain and adsorption of humidity (H₂O) molecule on the electronic structure and chemical activity of the in-plane graphene/silicene heterostructure. The considered heterostructure is found to be metallic with the Dirac point above the Fermi level, which can be shifted by applying either compressive or tensile strains. Moreover, the chemical activity of graphene/silicene heterostructure under the compressed (-7%) and tensile (7%) strains is found to be significantly large in comparison with that of its flat counterpart. The analysis is also conducted on the effect of the BN-substrate on the adsorption energies and the charge transfer between the graphene/silicene heterostructure and the adsorbed H₂O molecule. It shows that the BN-substrate significantly influences the donor/acceptor ability of H₂O molecule upon its adsorption on the graphene/silicene heterostructure and may cause an increase/decrease of the charge transfer between the H₂O molecule and heterostructure. The present study provides new knowledge on the properties of the in-plane graphene/silicene heterostructure and reveals the effects of strain and H₂O molecules on its electronic and chemical properties, which may be useful for its potential device applications.

2. Computational methods

All the calculations are based on the density functional theory (DFT) and performed by spin-polarized first-principles calculations. Vienna *ab initio* simulation package (VASP) [38] with the Perdew-Burke-Ernzerhof (PBE) functional [39] under the generalized gradient approximation (GGA) is used. The van der Waals (vdW) corrected functional with Becke88 optimization (optB88) [40] is selected to analyze dispersive interactions during the noncovalent chemical functionalization of structures with small molecules. All the structures are fully relaxed until the total energy and atomic forces were smaller than 10^{-5} eV and 0.01 eV/Å, respectively.

The free-standing graphene/silicene heterostructure is created by using the $5 \times 5 \times 1$ and $3 \times 3 \times 1$ supercells of graphene and silicene (60 carbon and 24 silicon atoms), respectively. To create BN-supported graphene/silicene heterostructure the initial free-standing heterostructure is placed on the BN-substrate. The substrate is created by using the $5 \times 11 \times 1$ supercell (60 boron and 60 nitride atoms). Periodic boundary conditions are applied in the two in-plane transverse directions, while the vacuum space of 20 Å is introduced

along the out-of-plane direction. Due to the difference between the lattice spacing of graphene (a_{gr}) and that of silicene (a_{si}), the mismatch strain along the interface of the graphene/silicene heterostructure is $\epsilon_{mismatch} = (5a_{gr} - 3a_{si})/(5a_{gr}) \approx 2.7\%$. Since during the relaxation, the supercell period along the zigzag direction is taken as $5a_{gr}$, the strain along the interface direction in the graphene is $\epsilon_{gr} = 0\%$, and that in the silicene is $\epsilon_{si} = \epsilon_{mismatch}$. The compressed/stretched structure is obtained by applying uniaxial strain in the direction perpendicular to the interface of the graphene/silicene heterostructure. The choice of the asymmetric graphene/silicene interface is based on previous works [41, 42] of in-plane heterostructures, where epitaxy of graphene with other 2D material occurs preferentially along the zigzag direction.

The first Brillouin zone is sampled with a $10 \times 10 \times 1$ k-mesh grid. The kinetic energy cutoff of 450 eV is adopted. The adsorption energy E_a of a molecule on the free-standing and BN-substrated graphene/silicene heterostructure is calculated as $E_a = E_{Mol+H} - E_{Mol} - E_H$, where E_{Mol+H} , E_{Mol} and E_H are the energies of the free-standing/BN-supported molecule adsorbed graphene/silicene heterostructure, molecule, and the free-standing/BN-supported graphene/silicene sheet, respectively. The electronic interaction between the H₂O molecule with graphene/silicene heterostructure is analyzed by differential charge density (DCD) $\Delta\rho(r)$ defined as the difference between the total charge density of the molecular-adsorbed graphene/silicene system and the sum of the charge densities of the isolated molecule and the planar graphene/silicene heterostructure. The exact amount of charge transfer between the molecule and the surface, the plane-averaged DCD $\Delta\rho(z)$ along the normal direction z of the graphene/silicene surface, is calculated by integrating $\Delta\rho(r)$ over the basal plane at the z point. The amount of transferred charge at the z point is given by $\Delta Q(z) = \int_{-\infty}^z \Delta\rho(z') dz'$. Based on the $\Delta Q(z)$ curves, the total amount of charge donated by the molecule is read at the interface between the molecule and the graphene/silicene where $\Delta\rho(z)$ shows a zero value. The geometric structures and charge density distributions are plotted through Visualization for Electronic and Structural Analysis (VESTA) [43].

3. Results and discussion

3.1 Strain effect on the electronic structure

Figures 1(a) – (e) present the variation of band gap of the in-plane graphene/silicene heterostructure under the tension strain of 7% and 5%, planar structure (0% of strain), and under the compressive strain of -5% and -7%, respectively, along the armchair direction. It is seen that the heterostructure remains a metal within the strain

range as there is no band gap near the Fermi level. For each considered case, the Dirac point is located above the Fermi level, signifying a p-type of conduction.

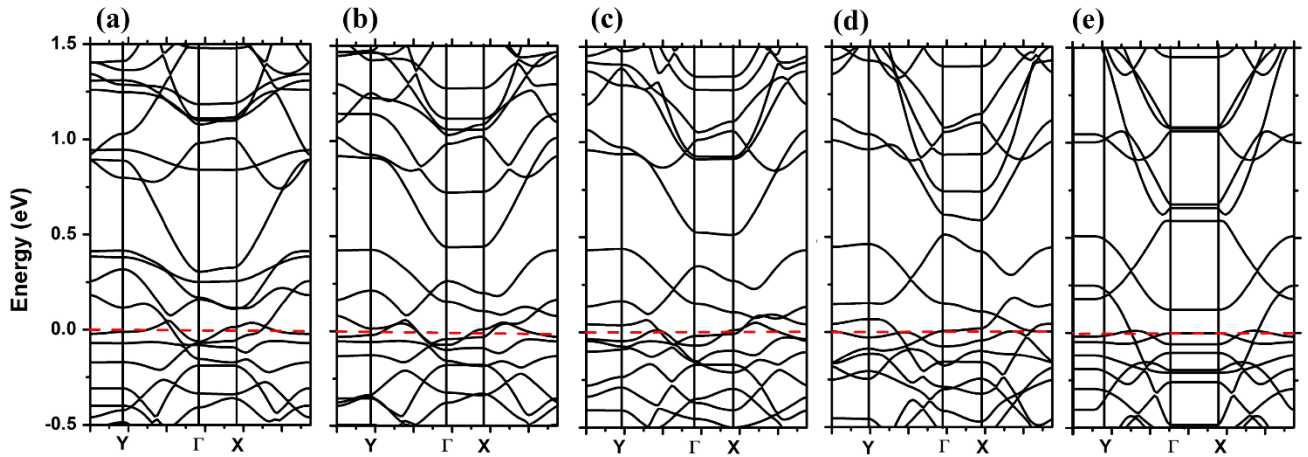


Figure 1. Variation of band gap of in-plane graphene/silicene heterostructure under different strains applied along the armchair direction (a)-(e). The applied strains are (a) 7%, (b) 5%, (c) 0%, (d) -5% and (e) -7%, respectively.

3.2 Interaction with environmental H₂O molecule

The adsorption of the environmental H₂O molecule on the graphene, silicene, and graphene/silicene interfacial regions of the in-plane graphene/silicene surface is considered. For each case, several possible symmetric anchoring positions of the molecule on the planar and compressed surfaces are examined. All subsequent calculations on the electronic properties and energetics are based on the lowest-energy configurations of the adsorbed heterostructure. The most stable configurations for the case of H₂O molecule adsorbed on the planar sheet are given in figures 2(a), (d) and (j). In case of H₂O adsorbed on the graphene region (figure 2(a)), both of the O–H bonds are disposed at the angle of around 45° to the surface and located directly above the ridge of graphene. The distance from the molecule to the surface is 2.87 Å, and the value of E_a is –0.152 eV, which is consistent with the result reported in [44]. Figure 2(d) shows the H₂O molecule adsorbed on silicene region, in which one of the O–H bonds is parallel to the surface along the armchair direction and the other nearly normal to the surface. The distance from the molecule to the surface is 2.89 Å, and E_a is –0.140 eV, which is in consistent with result in [45]. Figure 2(j) presents the H₂O adsorbed on the graphene/silicene region. It is seen that the molecule is located directly above the ridge of the graphene/silicene site, both O–H bonds are nearly parallel to the surface, the distance between the molecule and the surface is 2.71 Å, and E_a is –0.175 eV.

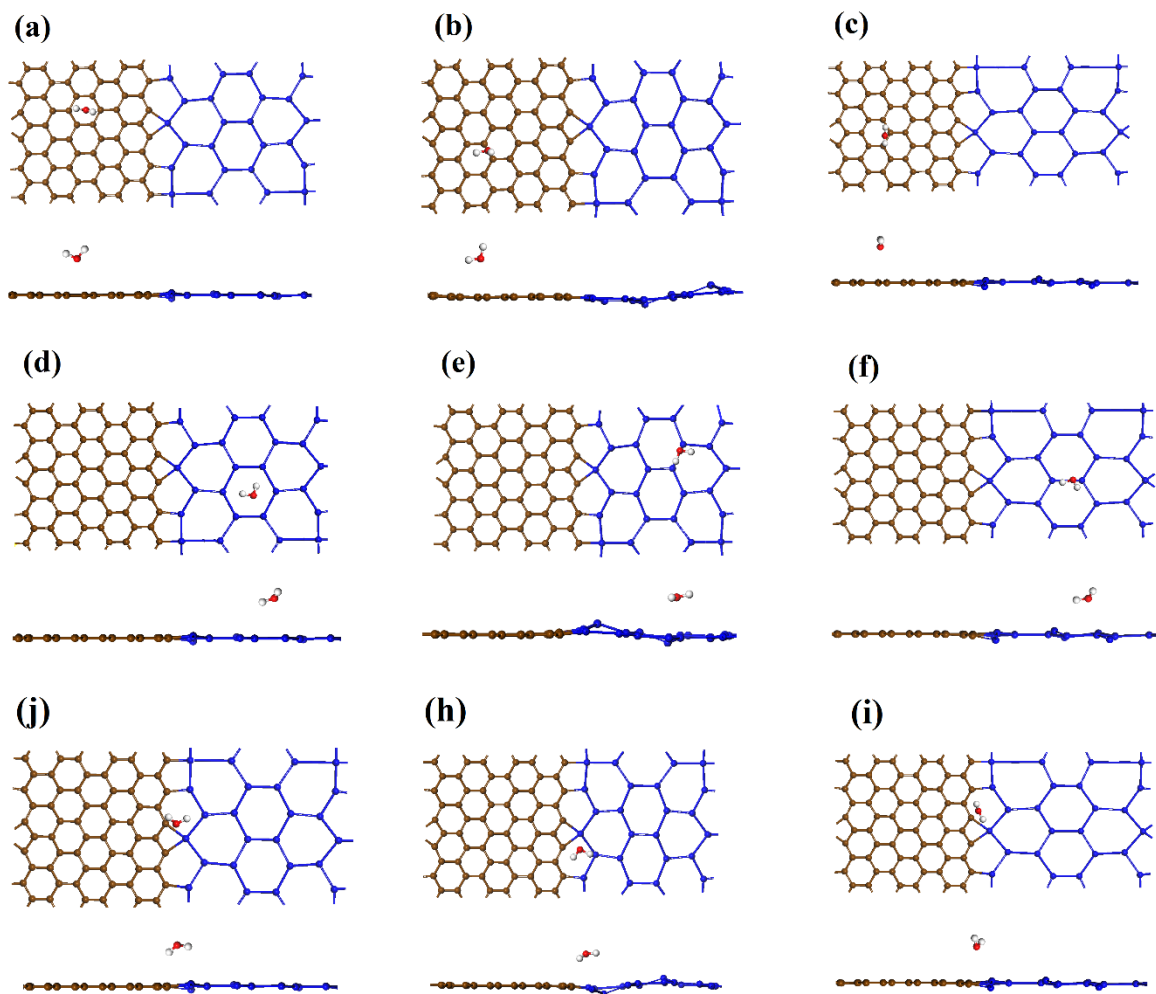


Figure 2. The most stable adsorption positions of the H₂O molecule on different regions of the heterostructure. Under 0% strain: (a) graphene region, (d) silicene region, and (j) the graphene/silicene interfacial region. Under -7% strain: (b) graphene region, (e) silicene region, and (h) the graphene/silicene interfacial region. Under 7% strain: (c) graphene region, (f) silicene region, and (i) the graphene/silicene interfacial region, respectively. The balls in brown, blue, white and red represent carbon, silicon, hydrogen and oxygen atoms, respectively.

For the H₂O adsorbed on the graphene/silicene sheet under the compressed strain of -7%, the most stable configurations are given in figures 2(b), (e) and (h). Figure 2(b) shows the H₂O adsorbed on the graphene region, in which the in-plane O–H bond is parallel to the surface along the armchair direction while the out-of-plane O–H bond is nearly normal to the surface and located directly above the armchair C–C bond. The distance from the molecule to the surface is 2.97 Å, and the value of E_a is -0.157 eV. In the case of the H₂O adsorbed on the silicene region (figure 2(e)), both O–H bonds are parallel to the surface and located directly above the zigzag Si–Si bond. The distance from the molecule to the surface is 2.82 Å, and E_a is -0.175 eV. Figure 2(h) presents the H₂O adsorbed on the graphene/silicene interfacial region, in which the molecule is located directly above the ridge of the graphene/silicene site and both of the O–H bonds are nearly parallel to surface, the distance between the molecule and the surface is 2.40 Å, and E_a is -0.210 eV.

For the H₂O adsorbed on the graphene/silicene sheet under the tensile strain of 7%, the most stable configurations are given in figures 2(c), (f) and (i). Figure 2(c) shows the H₂O adsorbed on the graphene region, in which the O–H bonds are disposed at the angle of around 45° to the surface and located directly above the armchair C–C bonds. The distance from the molecule to the surface is 3.03 Å, and the value of E_a is –0.145 eV. In the case of the H₂O adsorbed on the silicene region (figure 2(f)), both O–H bonds are parallel to the surface and located directly above the armchair Si–Si bond. The distance from the molecule to the surface is 2.72 Å, and E_a is –0.154 eV. Figure 2(i) presents the H₂O adsorbed on the graphene/silicene interfacial region, in which the molecule is located directly above the ridge of the graphene/silicene site and both of the O–H bonds are nearly parallel to surface, the distance between the molecule and the surface is 2.61 Å, and E_a is –0.160 eV.

It is found that in the case of the compressive strain the adsorption energy E_a increases with strain. A large enhancement is observed for the cases of H₂O adsorption on the silicene and graphene/silicene interfacial regions, which may be explained by the large distortion of the silicene lattice and Si-Si bonds deformation [46]. Tensile strain leads to the decrease of the adsorption energy E_a in the cases of the H₂O molecule adsorption on the graphene and interfacial graphene/silicene regions, while increases in the case when H₂O adsorbed on the silicene region. Table 1 summarizes the energetics data of the H₂O molecular adsorption.

Table 1. Adsorption energy (E_a) and charge transfer (Δq) from H ₂ O molecules to different regions of the planar, compressed and stretched graphene/silicene heterostructure, as well as the X–H bond length (B_{X-H}), where X represents the H ₂ O molecule. Note that a positive Δq indicates the transfer of electrons from the molecules to the graphene/silicene heterostructure.					
Strain	Heterostructure regions	E_a (eV)	Δq (e)	B_{X-H} (Å)	Molecule
0%	graphene	-0.152	0.024	2.87	donor
	silicene	-0.140	-0.092	2.89	acceptor
	graphene/silicene	-0.175	-0.057	2.71	acceptor
-7%	graphene	-0.157	0.035	2.97	donor
	silicene	-0.175	0.181	2.82	donor
	graphene/silicene	-0.210	-0.355	2.67	acceptor
7%	graphene	-0.145	-0.028	3.03	acceptor
	silicene	-0.154	0.160	2.72	donor
	graphene/silicene	-0.160	-0.050	2.61	acceptor

To gain insight into the electronic properties of the planar (under 0% strain), compressed (under the strain of -7%) and stretched (under the strain of 7%) graphene/silicene heterostructure after H₂O doping, we study the local density of states (LDOS). The LDOS analysis reveals that the additional electronic states induced by H₂O are located below the Fermi level for the molecular adsorption on planar, compressed or stretched surfaces (figure 3). However, the alignment of the molecular levels of H₂O is strongly dependent on the region of molecular adsorption and also affected by strain.

Figures 3(a), (d) and (j) present the three highest occupied molecular orbitals 1b₁ (HOMO), 3a₁ (HOMO-1), and 1b₂ (HOMO-2) of the H₂O molecule adsorbed, respectively, on the graphene, silicene and graphene/silicene interfacial regions of the planar sheet. Clearly, the distributions of molecular orbitals are different for each region of the heterostructure. Moreover, by comparing the planar, compressed and stretched structures of silicene (as shown in figures 3(b), (e) and (h), respectively) and the graphene/silicene interfacial region (figures 3(c), (f) and (i)), we see that 1b₁, 3a₁, and 1b₂ molecular orbitals of the H₂O molecule are shifted downwardly by around 0.25 eV for the cases when the compressive or tensile strains are applied.

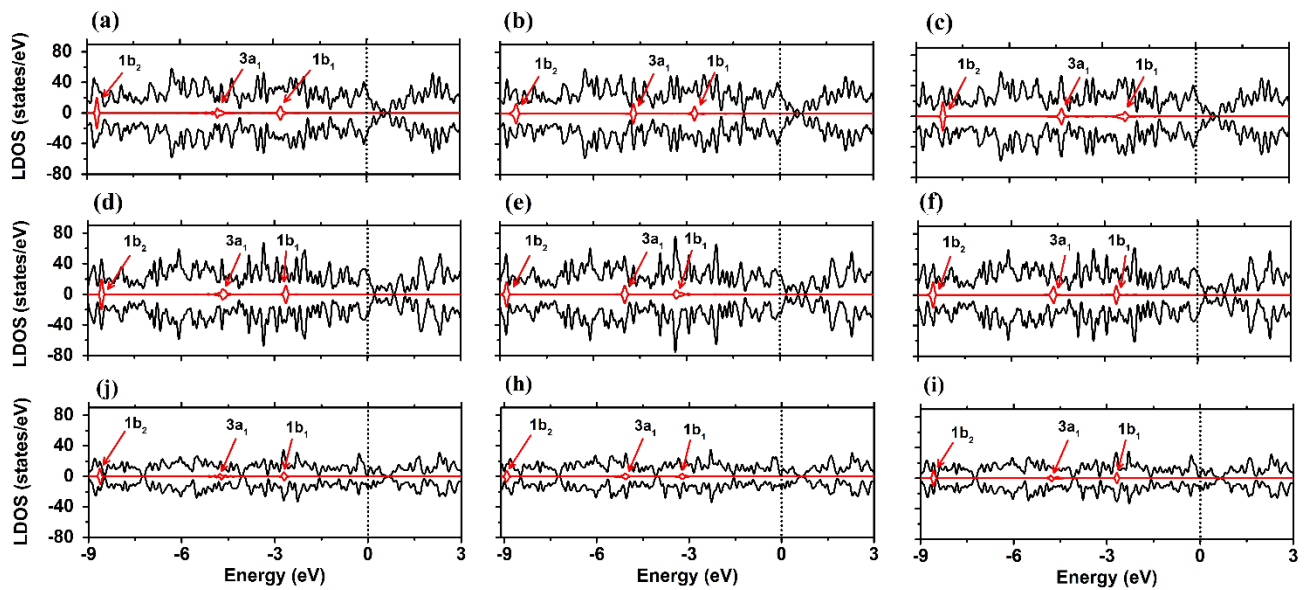


Figure 3. LDOS of the H₂O molecule on different regions of the heterostructure. Under 0% strain: (a) graphene region, (e) silicene region, and (c) the graphene/silicene interfacial region. Under -7% strain: (g) graphene region, (d) silicene region, and (f) the graphene/silicene interfacial region. Under 7% strain: (j) graphene, (h) silicene, and (i) the graphene/silicene interfacial region, respectively. The spin-up and -down bands for H₂O are the same and shown by the red line, while the black line represents the total DOS.

3.3 Modulation of carrier density and charge transfer

To analyze the electronic interaction of the graphene/silicene heterostructure with the H₂O molecule, the DCD $\Delta\rho(r)$ is calculated. The isosurfaces of the $\Delta\rho(r)$ for the H₂O molecule adsorbed on the different regions of the graphene/silicene heterostructure under 0%, -7% and 7% strains are depicted in figures 4(a)-(c), 5(a)-(c) and 6(a)-(c), respectively.

For the planar surface, there is a depletion of electrons in the H₂O molecule and an accumulation of electrons in the nearest C atoms within the graphene region (figure 4(a)). The H₂O molecule clearly donates electrons to the graphene with around 0.024 e per molecule. This result is consistent with the previous DFT study [44], where H₂O was found to be a donor on graphene. However, in a real experiment, the adsorbed water shows the acceptor character [47] due to the time-average behavior of water adsorption with more binding possibilities. The charge-transfer analysis for the H₂O adsorbed on the silicene region of the planar structure (figure 4(b)) shows that the molecule accepts about 0.092 e . In the case when the H₂O adsorbed on the planar graphene/silicene interfacial region (figure 4(c)), the total amount of transferred charge is -0.057 e . Interestingly, electrons accumulate in the nearest C atoms, while the Si atoms donate electrons to the H₂O.

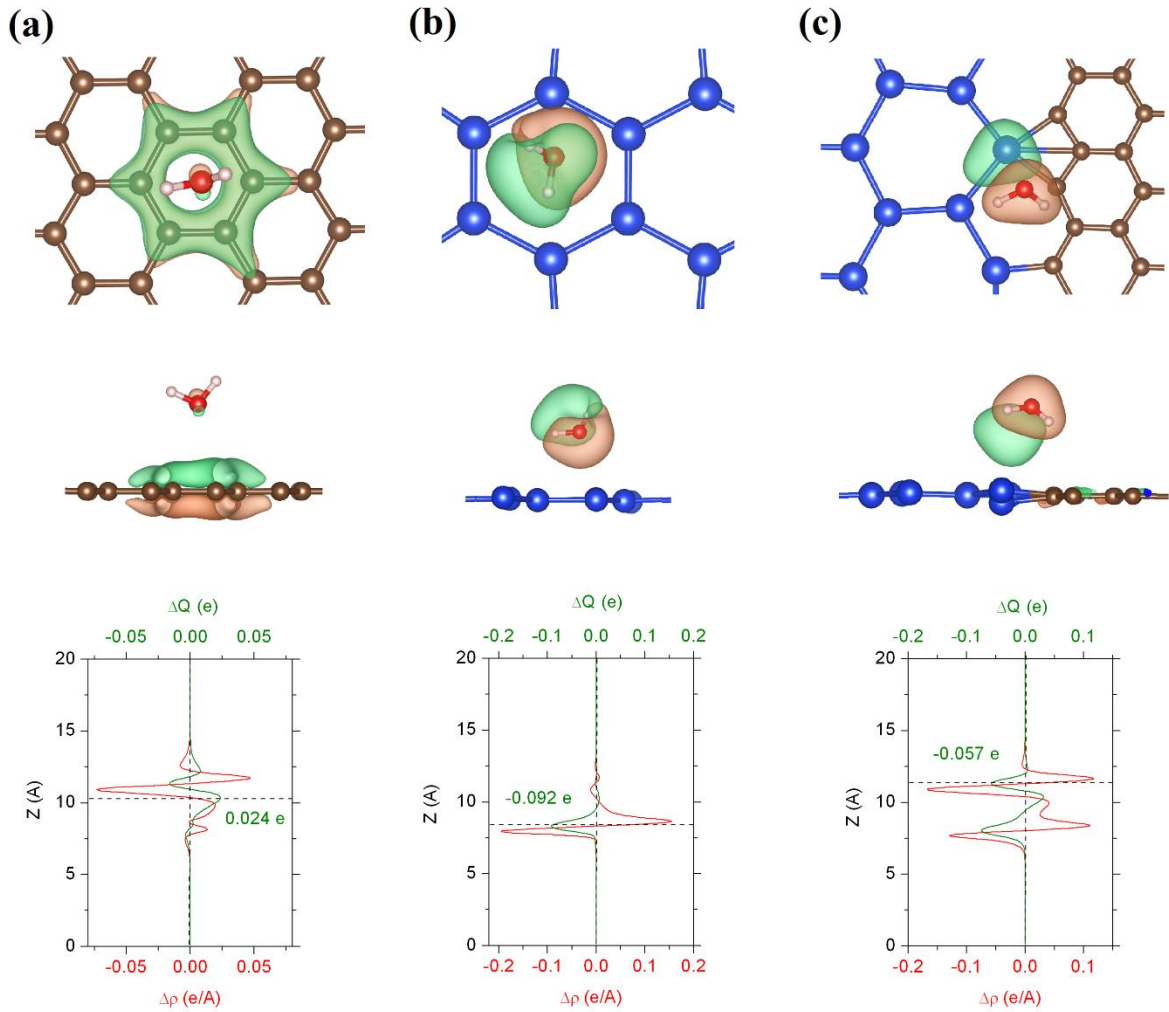


Figure 4. Top and side views of the 0.02\AA^{-3} DCD isosurface (the green/orange color denotes depletion/accumulation of electrons), the plane-averaged DCD $\Delta\rho(z)$ (red line) and the amount of transferred charge $\Delta Q(z)$ (green line) for the H_2O molecule adsorbed on (a) graphene, (b) silicene, and (c) graphene/silicene interfacial regions of the planar graphene/silicene sheet.

The compressive strain of -7% leads to an increase in the chemical activity of the H_2O molecule, and the total amount of transferred charge from the molecule to the C atoms of the graphene region (figure 5(a)) is $0.035 e$. Figure 5(b), where the H_2O is adsorbed in the silicene region of the compressed structure, clearly indicates an accumulation of electrons in the Si atoms. Thus, H_2O serves as a donor in this case where charge transfer from the molecule to the surface is $0.181 e$. A significant increase of the charge transfer, up to $-0.355 e$, is found for the case of H_2O adsorption on the interfacial region of the compressed structure (figure 5(c)), and the main charge transfer is still observed for the C atoms. The obtained results suggest that the carrier density and the charge transfer between the H_2O molecule and different regions of the in-plane graphene/silicene heterostructure, as well as a donor/acceptor ability of the H_2O , can be significantly tuned by compressive strain.

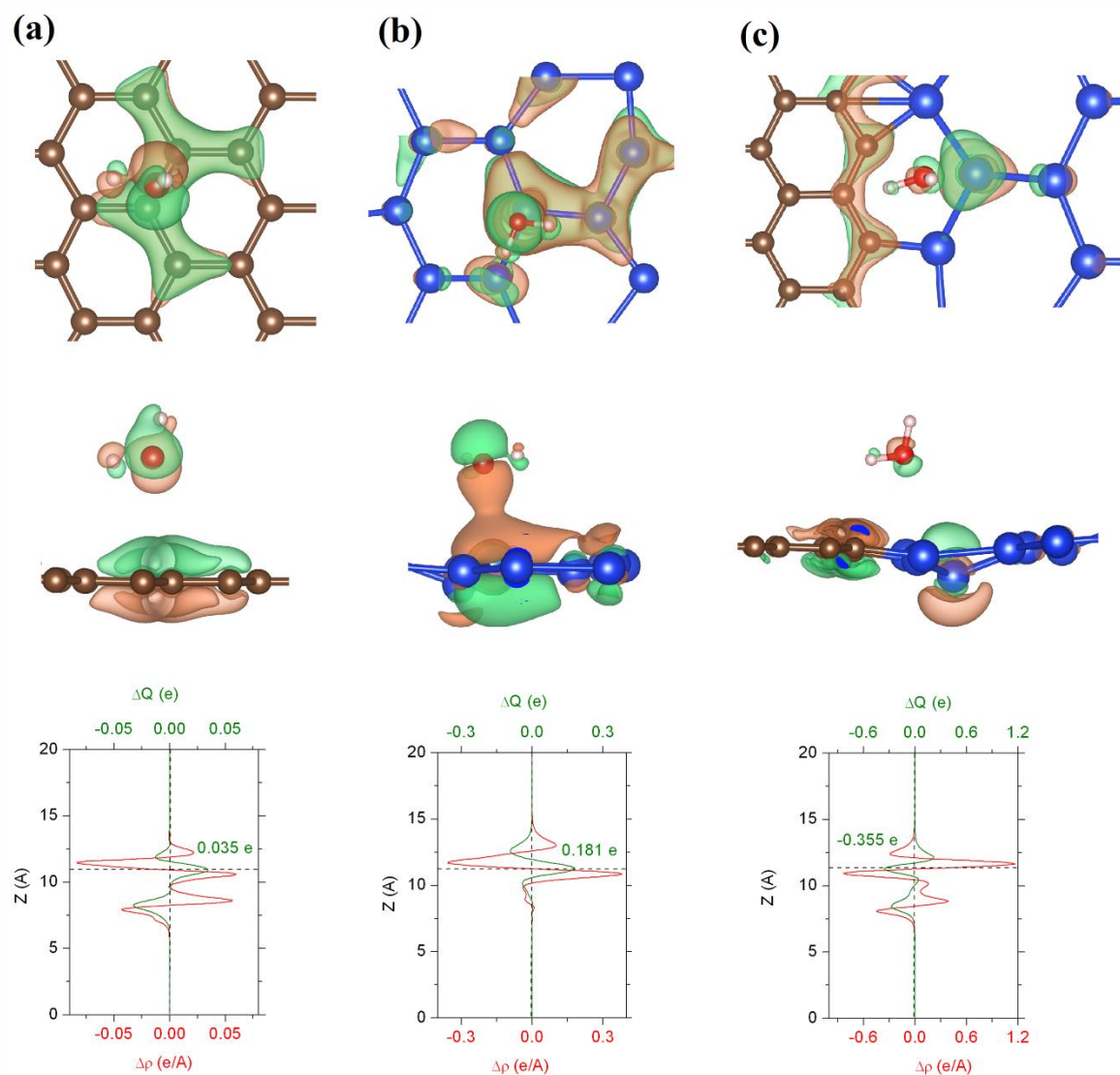


Figure 5. Top and side views of the 0.035\AA^{-3} DCD isosurface (the green/orange color denotes depletion /accumulation of electrons), the plane-averaged DCD $\Delta\rho(z)$ (red line), and the amount of transferred charge $\Delta Q(z)$ (green line) for the H_2O molecule adsorbed on (a) graphene, (b) silicene, and (c) graphene/silicene interfacial regions of the compressed graphene/silicene sheet.

The tensile strain of 7% also leads to the change in the chemical activity of the H_2O molecule. In particular, the total amount of transferred charge from the C atoms of the graphene region to the molecule (figure 6(a)) is 0.028 e , clearly indicating that H_2O serves as an acceptor. Figure 6(b), where the H_2O is adsorbed on the silicene region of the stretched structure, indicates that molecule donates about 0.160 e to the surface, signifying that H_2O serves as a donor. For the case of H_2O adsorption on the interfacial region of the stretched structure (figure 6(c)) the main charge transfer, up to 0.050 e , is still observed for the H_2O molecule. The obtained results suggest that the carrier density and the charge transfer between the H_2O molecule and different regions of the in-plane graphene/silicene heterostructure, as well as a donor/acceptor ability of the H_2O , can be tuned by tensile strain.

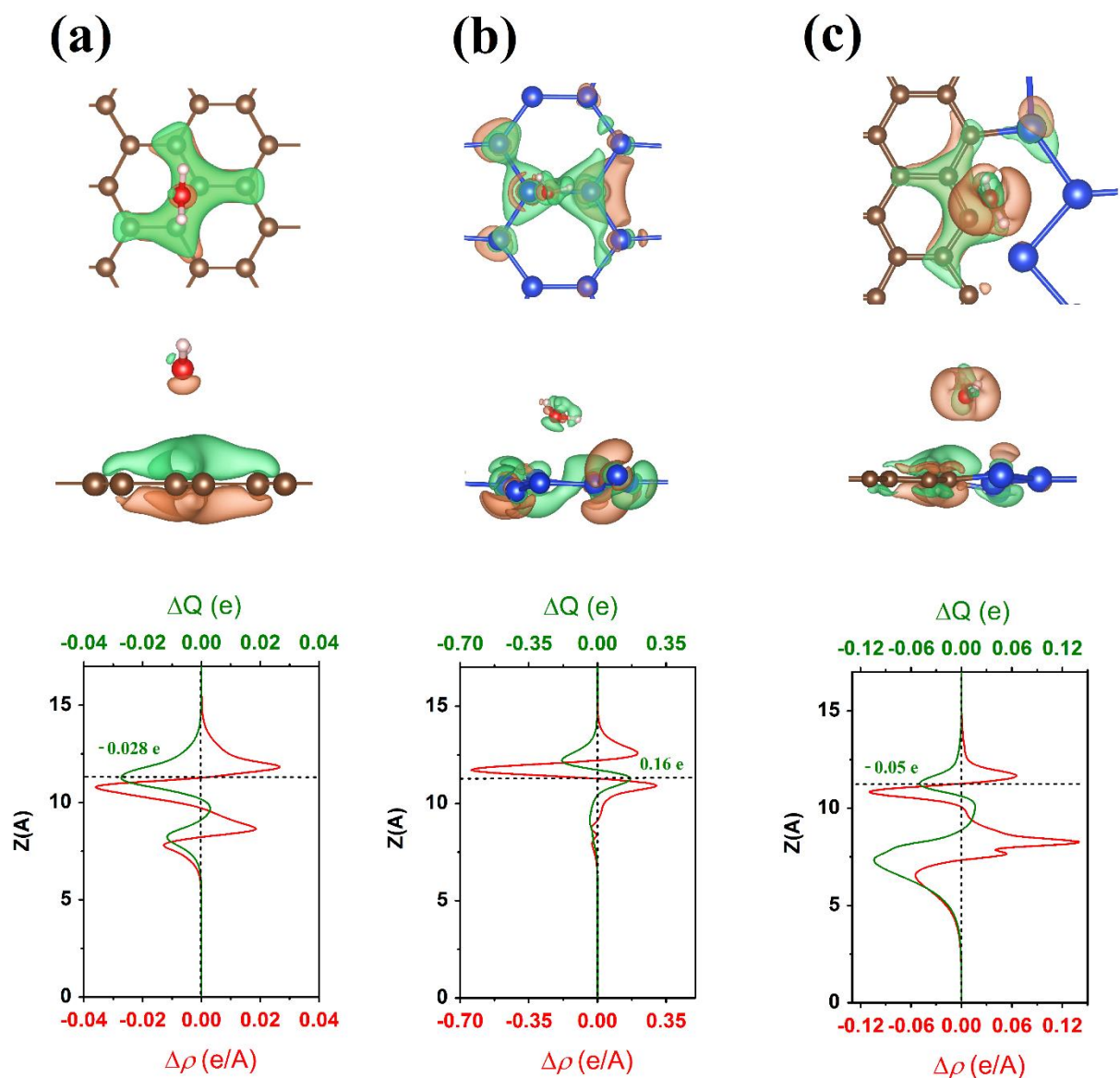


Figure 6. Top and side views of the 0.015\AA^{-3} DCD isosurface (the green/orange color denotes depletion /accumulation of electrons), the plane-averaged DCD $\Delta\rho(z)$ (red line), and the amount of transferred charge $\Delta Q(z)$ (green line) for the H_2O molecule adsorbed on (a) graphene, (b) silicene, and (c) graphene/silicene interfacial regions of the stretched graphene/silicene sheet.

3.4 The effects of the BN-substrate on the chemical activity of the graphene/silicene heterostructure

To understand the effect of substrate on the chemical activity of the graphene/silicene heterostructure, we choose the h-BN monolayer as a substrate [48, 49]. Specifically, we focus on how the substrate affects the adsorption energies and the charge transfer between the graphene/silicene heterostructure and the adsorbed H_2O molecule. For the heterostructure supported by the substrate without applying strain, the most stable configurations for the H_2O molecule adsorbed on different regions of the heterostructure are given in figures 7(a), (b) and (c), respectively.

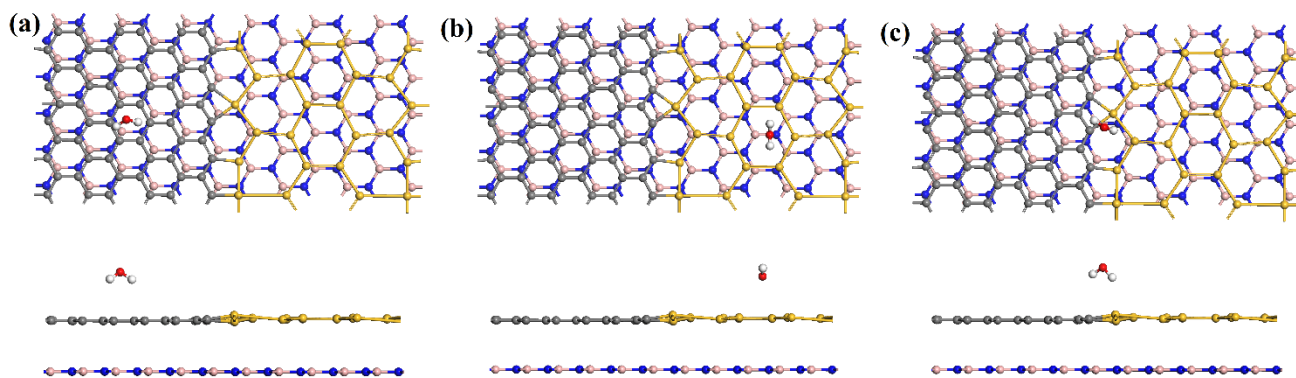


Figure 7. The most stable adsorption positions of the H₂O molecule on the graphene/silicene heterostructure supported by the BN layer without applying strain: (a) graphene, (b) silicene, and (c) the graphene/silicene interfacial regions. The balls in gray, yellow, white, red, blue and pink represent carbon, silicon, hydrogen, oxygen, nitrogen and boron atoms, respectively.

In the case of H₂O adsorbed on the graphene region (figure 7(a)), both of the O–H bonds are disposed at the angle of around 45° to the surface and located directly above the ridge of graphene, which is similar to the case in which H₂O is adsorbed on the graphene region of the free-standing surface. The value of E_a is –0.152 eV and the total amount of transferred charge from the molecule to the surface is 0.024 e. Figure 7(b) shows the H₂O molecule adsorbed on the silicene region of the substrate-supported heterostructure, in which the O–H bonds are disposed at the angle of around 45° to the surface and located directly above the ridge of silicene. The value of E_a is –0.140 eV and the total amount of transferred to the molecule is 0.092 e. Figure 7(c) presents the H₂O adsorbed on the graphene/silicene region. It is seen that the molecule is located directly above the C–Si bond of the graphene/silicene site, and both O–H bonds are disposed at the angle of around 45° to the surface. The value of E_a is –0.175 eV and the total amount of transferred to the molecule is 0.057 e.

It is found that the BN-substrate has a small effect on the adsorption energy E_a , when H₂O molecule is adsorbed on the graphene region of the graphene/silicene heterostructure. However, for the substrate-supported heterostructure, the E_a is slightly higher for the case of H₂O adsorbed on the silicene region and significantly lower for the case where H₂O is adsorbed on the graphene/silicene interfacial regions, compared with the E_a of the free-standing heterostructure. The charge transfer analysis reveals that the presence of the BN-substrate significantly influences the donor/acceptor ability of H₂O molecule upon its adsorption on the graphene/silicene heterostructure and may cause an increase/decrease of the charge transfer between the H₂O molecule and the heterostructure. Table 2 summarizes the energetics data of the H₂O molecular adsorption on the substrate-supported and free-standing graphene/silicene heterostructure.

Table 2. Adsorption energy (E_a) and charge transfer (Δq) from H ₂ O molecules to different regions of the planar free-standing and BN-supported graphene/silicene heterostructure. Note that a positive Δq indicates the transfer of electrons from the molecules to the graphene/silicene heterostructure.				
Graphene/silicene heterostructure	Heterostructure regions	E_a (eV)	Δq (e)	Molecule
On the BN-substrate	graphene	-0.152	0.024	donor
	silicene	-0.140	-0.092	acceptor
	graphene/silicene	-0.175	-0.057	acceptor
Free-standing	graphene	-0.146	-0.014	acceptor
	silicene	-0.150	0.011	donor
	graphene/silicene	-0.144	-0.022	acceptor

4. Conclusions

By using the first-principles calculations the strain effects on the electronic structure of the in-plane graphene/silicene heterostructure are studied. Within the strain range from -7% (compression) to 7% (tension) the considered heterostructure is always metallic with the Dirac point being located above the Fermi level.

The investigation of the strain effects on the chemical activity of the in-plane graphene/silicene heterostructure upon interaction with H₂O molecule reveals that compressive strain is able to promote the adsorption of H₂O molecule and increase the charge transfer, signifying an enhanced chemical activity. Furthermore, compressive and tensile strains are found to be able to modulate the charge transfer between the H₂O molecule and graphene/silicene surface, potentially allowing the control of polarity and concentration of charge carriers. In addition, the effect of the BN-substrate on the chemical activity of the in-plane graphene/silicene heterostructure upon interaction with the H₂O molecule is considered. It is found that the BN-substrate significantly influences the donor/acceptor ability of H₂O molecule upon its adsorption on the graphene/silicene heterostructure and may cause an increase/decrease of the charge transfer between the H₂O molecule and heterostructure. This study provides deep insights into the effects of strain and water molecule on the electronic properties and chemical activity of the in-plane graphene/silicene heterostructure, which may be useful for its potential device applications.

ACKNOWLEDGMENTS

The authors gratefully acknowledge the financial support from the Ministry of Education, Singapore (Academic Research Fund TIER 1 – RG128/14), the Agency for Science, Technology and Research (A*STAR), Singapore, and the use of computing resources at the A*STAR Computational Resource Centre, Singapore. This work was supported in part by a grant from the Science and Engineering Research Council (152-70-00017). Sergey V. Dmitriev acknowledges financial support from the Russian Science Foundation grant N 14-13-00982.

REFERENCES

- [1]. K. S. Novoselov, A. K. Geim, S. V. Morozov, D. Jiang, Y. Zhang, S. V. Dubonos, I. V. Grigorieva and A. A. Firsov, Electric field effect in atomically thin carbon films, *Science*, 2004, **306**, 666–669.
- [2]. K. I. Bolotin, K. J. Sikes, Z. Jiang, M. Klima, G. Fudenberg, J. Hone, P. Kim and H. L. Stormer, Ultrahigh electron mobility in suspended graphene, *Solid State Commun.*, 2008, **146**, 351–355.
- [3]. C. Lee, X. Wei, J. W. Kysar and J. Hone, Measurement of the elastic properties and intrinsic strength of monolayer graphene, *Science*, 2008, **321**, 385–388.
- [4]. S.-M. Choi, S.-H. Jhi and Y. W. Son, Effects of strain on electronic properties of graphene, *Phys. Rev. B*, 2010, **81**, 081407.
- [5]. L. Tao, E. Cinquanta, D. Chiappe, C. Grazianetti, M. Fanciulli, M. Dubey, A. Molle and D. Akinwande, Silicene field-effect transistors operating at room temperature, *Nat. Nano.*, 2015, **10**, 227.
- [6]. D. Jose and A. Datta, Structures and chemical properties of silicene: unlike graphene, *Acc. Chem. Res.*, 2014, **47**, 593–602.
- [7]. Z. G. Shao, X. S. Ye, L. Yang and C. L. Wang, First-principles calculation of intrinsic carrier mobility of silicene, *J. Appl. Phys.*, 2013, **114**, 093712.
- [8]. Q. X. Pei, Z. D. Sha, Y. Y. Zhang, Y.-W. Zhang, Effects of temperature and strain rate on the mechanical properties of silicene, *J. Appl. Phys.*, 2014, 115, 023519.
- [9]. S. Park, C. Park and G. Kim, Interlayer coupling enhancement in graphene/hexagonal boron nitride heterostructures by intercalated defects or vacancies, *J. Chem. Phys.*, 2014, **140**, 134706.
- [10]. Y. Cai, G. Zhang and Y.-W. Zhang, Electronic properties of phosphorene/graphene and phosphorene/hexagonal boron nitride heterostructures, *J. Phys. Chem. C*, 2015, **119**, 13929–13936.
- [11]. W. J. Yu, Y. Liu, H. Zhou, A. Yin, Z. Li, Y. Huang and X. Duan, Highly efficient gate-tunable photocurrent generation in vertical heterostructures of layered materials, *Nature Nano.*, 2013, **8**, 952–958.

- [12]. Z. Wang, Q. Chen and J. Wang, Electronic structure of twisted bilayers of graphene/MoS₂ and MoS₂/MoS₂. *J. Phys. Chem. C*, 2015, **119**, 4752–4758.
- [13]. Y. Cai, Q. X. Pei, G. Zhang and Y.-W. Zhang, Decoupled electron and phonon transports in hexagonal boron nitride-silicene bilayer heterostructure, *J. Appl. Phys.*, 2016, **119**, 065102.
- [14]. W. Hu, Z. Li and J. Yang, Structural, electronic, and optical properties of hybrid silicene and graphene nanocomposite. *J. Chem. Phys.*, 2013, **139**, 154704.
- [15]. A. K. Geim and I. V. Grigorieva, Van der Waals heterostructures, *Nature*, 2013, **499**, 419–425.
- [16]. Z. Yin, X. Zhang, Y. Cai, J. Chen, J. I. Wong, Y. Y. Tay, J. Chai, J. Wu, Z. Zeng, B. Zheng, H. Y. Yang and H. Zhang, Preparation of MoS₂–MoO₃ hybrid nanomaterials for light-emitting diodes, *Angew. Chem.*, 2014, **126**, 1–7.
- [17]. H. Wang, F. Liu, W. Fu, Z. Fang, W. Zhou and Z. Liu, Two dimensional heterostructures: Fabrication, characterization, and application. *Nanoscale*, 2014, **6**, 12250–12272.
- [18]. Y. Deng, Z. Luo, N. J. Conrad, H. Liu, Y. Gong, S. Najmaei, P. M. Ajayan, J. Lou, X. Xu and P. D. Ye, Black phosphorus-monolayer MoS₂ van der Waals heterojunction p-n diode, *ACS Nano*, 2014, **8**, 8292–8299.
- [19]. J. Yuan, S. Najmaei, Z. Zhang, J. Zhang, S. Lei, P. M. Ajayan, B. I. Yakobson and J. Lou, Photoluminescence quenching and charge transfer in artificial heterostacks of monolayer transition metal dichalcogenides and few-layer black phosphorus, *ACS Nano*, 2015, **9**, 555–563.
- [20]. Y. Cai, Q. Ke, G. Zhang and Y.-W. Zhang, Energetics, charge transfer and magnetism of small molecules physisorbed on phosphorene, *J. Phys. Chem. C*, 2015, **119**, 3102–3110.
- [21]. H. H. Gürel, V. O. Özçelik and S. Ciraci, Dissociative adsorption of molecules on graphene and silicene, *J. Phys. Chem. C*, 2014, **118**, 27574–27582.
- [22]. X. Ling, H. Wang, S. Huang, F. Xia and M. S. Dresselhaus, The renaissance of black phosphorus. *Proc. Natl. Acad. Sci. U. S. A.*, 2015, **112**, 4523–4530.
- [23]. G. R. Berdiyrov, M. Neek-Amal, F. M. Peeters and A. C. T. van Duin, Stabilized silicene within bilayer graphene: A proposal based on molecular dynamics and density-functional tight-binding calculations. *Phys. Rev. B*. 2014, **89**, 024107.
- [24]. S. J. Haigh, A. Gholinia, R. Jalil, S. Romani, L. Britnell, D. C. Elias, K. S. Novoselov, L. A. Ponomarenko, A. K. Geim and R. Gorbachev, Cross-sectional imaging of individual layers and buried interfaces of graphene-based heterostructures and superlattices, *Nature Mater.*, 2012, **11**, 764–767.
- [25]. Y. Wei, C. Guorui, S. Zhiwen, L. Cheng-Cheng, Z. Lianchang, X. Guibai, C. Meng, W. Duoming, Y. Rong, S. Dongxia, W. Kenji, T. Takashi, Y. Yugui, Z. Yuanbo and Z. Guangyu, Epitaxial growth of single-domain graphene on hexagonal boron nitride, *Nature Mater.*, 2013, **12**, 792–797.

- [26]. Y. Gong, J. Lin, X. Wang, G. Shi, S. Lei, Z. Lin, X. Zou, G. Ye, R. Vajtai, B. I. Yakobson, H. Terrones, M. Terrones, B. K. Tay, J. Lou, S. T. Pantelides, Z. Liu, W. Zhou and P. M. Ajayan, Vertical and in-plane heterostructures from WS₂/MoS₂ monolayers, *Nature Materials*, 2014, **13**, 1135–1142.
- [27]. Q. Sun, Y. Dai, Y. Ma, W. Wei and B. Huang, Lateral heterojunctions within monolayer h-BN/graphene: a first-principles study, *RSC Adv.*, 2015, **5**, 33037.
- [28]. Z. Huang, C. He, X. Qi, H. Yang, W. Liu, X. Wei, X. Peng and J. Zhong, Band structure engineering of monolayer MoS₂ on h-BN: First-principles calculations, *J. Phys. D: Appl. Phys.*, 2014, **47**, 075301.
- [29]. F. Withers, O. Del Pozo-Zamudio, A. Mishchenko, A. P. Rooney, A. Gholinia, K. Watanabe, T. Taniguchi, S. J. Haigh, A. K. Geim, A. I. Tartakovskii and K. S. Novoselov, Light-emitting diodes by band-structure engineering in van der Waals heterostructures, *Nature Materials*, 2015, **14**, 301–306.
- [30]. W. Pan, J. Xiao, J. Zhu, C. Yu, G. Zhang, Z. Ni, K. Watanabe, T. Taniguchi, Y. Shi and X. Wang, Biaxial compressive strain engineering in graphene/boron nitride heterostructures, *Scientific Reports*, 2012, **2**, 893, DOI: 10.1038/srep00893.
- [31]. A. Ramasubramaniam, D. Naveh and E. Towe, Tunable band gaps in bilayer graphene-BN heterostructures, *Nano Lett.*, 2011, **11**, 1070–1075.
- [32]. M. Brij, K. Ashok and P. K. Ahluwalia, Electronic and optical properties of silicene under uni-axial and bi-axial mechanical strains: A first principle study, *Physica E*, 2014, **61**, 40–47.
- [33]. C. Guoxin, Atomistic studies of mechanical properties of graphene, *Polymers*, 2014, **6**, 2404-2432.
- [34]. X. Li, L. Fan, Z. Li, K. Wang, M. Zhong, J. Wei, D. Wu and H. Zhu, Boron doping of graphene for graphene-silicon p-n junction solar cells, *Adv. Energy Mater.*, 2012, **2**, 425–429.
- [35]. H. Behera and G. Mukhopadhyay, Strain-tunable band gap in graphene/h-BN hetero-bilayer, *J. Phys. Chem. Solids*, 2012, **73**, 818–821.
- [36]. A. Ebnonnasir, B. Narayanan, S. Kodambaka and C. V. Ciobanu, Tunable MoS₂ bandgap in MoS₂-graphene heterostructures, *Appl. Phys. Lett.*, 2014, **105**, 031603.
- [37]. X. Liu and Z. Li, Electric field and strain effect on graphene-MoS₂ hybrid structure: Ab initio calculations, *J. Phys. Chem. Lett.*, 2015, **6**, 3269–3275.
- [38]. G. Kresse and J. Furthmüller, Efficient iterative schemes for ab initio total-energy calculations using a plane-wave basis set, *Phys. Rev. B: Condens. Matter Mater. Phys.*, 1996, **54**, 11169.
- [39]. J. P. Perdew, K. Burke and M. Ernzerhof, Efficient iterative schemes for ab initio total-energy calculations using a plane-wave basis set, *Phys. Rev. Lett.*, 1996, **77**, 3865–3868.
- [40]. A. D. Becke, Density-functional exchange-energy approximation with correct asymptotic behavior, *Phys. Rev. A: At., Mol., Opt. Phys.*, 1988, **38**, 3098.

- [41]. Y. Gong, J. Lin, X. Wang, G. Shi, S. Lei, Z. Lin, X. Zou, G. Ye, R. Vajtai, B. I. Yakobson et. al., Vertical and in-plane heterostructures from WS₂/MoS₂ monolayers, *Nature Materials*, 2015, **13**, 1135-1142.
- [42]. Y. Gao, Y. Zhang, P. Che, Y. Li, M. Liu, T. Gao, D. Ma, Y. Chen, Z. Cheng, X. Qiu, W. Duan, and Z. Liu, Towards single-layer uniform hexagonal boron nitride-graphene patchworks with zigzag linking edges, *Nano Lett.*, 2013, **13**, 3439-3443.
- [43]. K. Momma and F. Izumi, VESTA 3 for three-dimensional visualization of crystal, volumetric and morphology data, *J. Appl. Crystallogr.*, 2011, **44**, 1272-1276.
- [44]. O. Leenaerts, B. Partoens and F. M. Peeters, Adsorption of H₂O, NH₃, CO, NO₂, and NO on graphene: A first-principles study, *Phys. Rev. B*, 2008, **77**, 12541.
- [45]. W. Hu, Z. Li, J. Yang, Water on silicene: Hydrogen bond autocatalysis induced physisorption-chemisorption-dissociation transition, *arXiv:1603.04372*.
- [46]. Y. Wang and Y. Ding, Strain-induced self-doping in silicene and germanene from first-principles, *Solid State Comm*, 2013, **155**, 6-11.
- [47]. F. Schedin, A. K. Geim, S. V. Morozov, E. W. Hill, P. Blake, M. I. Katsnelson and K. S. Novoselov, Detection of individual gas molecules adsorbed on graphene, *Nat. Mater.*, 2007, **6**, 652.
- [48]. Q. H. Wang, Z. Jin, K. K. Kim, A. J. Hilmer, G. L. C. Paulus, C.-J. Shih, M.-H. Ham, J. D. Sanchez-Yamagishi, K. Watanabe, T. Taniguchi, J. Kong, P. Jarillo-Herrero and M. S. Strano, Understanding and controlling the substrate effect on graphene electron-transfer chemistry via reactivity imprint lithography, *Nat. Chem.*, 2012, **4**, 724-732.
- [49]. R. Li, Y. Hanac and J. Dong, Substrate effects on the monovacancies of silicene: studied from first principle methods, *Phys. Chem. Chem. Phys.*, 2015, **17**, 22969-22976.